Electronic Structure and Photoelectron Spectra of Bispentalene Complexes of Thorium and Uranium

F. Geoffrey N. Cloke,[†] Jennifer C. Green,*[,‡] and Christian N. Jardine[‡]

School of Chemistry, Physics and Environmental Science, University of Sussex, Brighton BN1 9QJ, U.K., and Inorganic Chemistry Laboratory, University of Oxford, South Parks Road, Oxford OX1 3QR, U.K.

Received September 21, 1998

The preparation of [U{η^8-C_8H_4(1,4-Si^{i}Pr$_3$)$_2$}$_2$] is reported. The binding of the pentalene ligand in an η^8 mode is examined by density functional calculations and photoelectron spectroscopy. Geometry optimization of [M(η^8-C_8H_6)$_2$], M = Th with D_{2d} and D_2 symmetry constraints, gives structures in good agreement with the X-ray structure found for [Th{η^8-C_8H_4(1,4-Si^{i}Pr$_3$)$_2$}$_2$]; in particular the folded nature of the ligand is well reproduced by the calculation. Examination of the barrier to relative rotation of the two ligands only showed a significant energy rise when the two rings were eclipsed. Geometry optimization for M = U, assuming D_{2d} symmetry and a triplet state, gave a structure similar to the Th compound but with shorter metal−carbon bond lengths. The two U f electrons were constrained to occupy degenerate orbitals of e symmetry. He I and He II spectra of [M{η^8-C_8H_4(1,4-Si^{i}Pr$_3$)$_2$}$_2$], M = Th and U, are presented and assigned with the aid of density functional calculations. The principal binding is by δ bonds between the upper occupied π orbitals of the pentalene dianion and the actinide d and f orbitals of appropriate symmetry.

Introduction

Because of its relative unavailability, the chemistry of the pentalene dianion, $C_8H_6^{2-}$ (pent^{2-}), has been studied far less than that of the other eight-membered aromatic dianion, $C_8H_8^{2-}$, derived from cyclooctatetraene. Transition metal complexes of pentalene have been reported, but in general these are η^5 complexes, with two metal atoms, each binding to a separate five-membered ring of the pentalene ligand in a trans conformation, e.g., [(η^3-C_3H_5)Ni(η^5,η^5-C_8H_6)Ni(η^3-C_3H_5)][1] and [(η^5-C_5Me_5)M(η^5,η^5-C_8H_6)M(η^5-C_5Me_5)] (M = Fe, Co, Ni).[2] Cis modes of bonding to two metals, where there is no direct bonding between the metals, have also been observed, e.g. [{Ru(MMe$_3$)(CO)$_2$}$_2$(η^5,η^5-C_8H_6)] (M = Si, Ge), [Ru$_3$(CO)$_8$(η^5,η^5-C_8H_6)].[3] The cis complexes cause a folding of the pentalene ligand by approximately 10°, which relieves steric interaction between the groups bound to the metals. In the case of the metal−metal bonded dimer, Mo$_2$(η^5,η^5-C_8H_4{1,4-Si^{i}Pr$_3$}$_2$)$_2$, the pentalene ligands are effectively planar.[4] For η^8 bonding to a single metal, the wingtip carbons must interact with the metal. This necessitates a folding of the ligand toward the metal, which must be stabilized by a bonding interaction to counteract the loss of aromaticity in the ring. Because of their size and exemption from the 18-electron rule, it has been suggested that f-block compounds would be the most likely to produce η^8 pentalene complexes,[5] although early transition metals with their low electron numbers may also fulfill these criteria. Indeed, the novel compound [Th(η^8-C_8H_4{1,4-Si^{i}Pr$_3$}$_2$)$_2$] has been prepared by Cloke,[5] while V(η^8-C_8H_6)(η^5-C_5H_5),[6] MCl(η^8-C_8H_6) (η^5-C_5H_5) (M = Ti, Zr), and Ti(η^8-C_8H_6)$_2$[7] have been reported by Jonas et al.

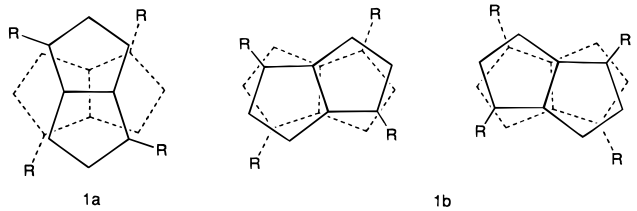

Figure 1. Isomers of M(η^8-C_8H_4{1,4-Si^{i}Pr$_3$}$_2$)$_2$. 1a shows a projection with near S_4 symmetry. 1b shows projections of two enantiomers with D_2 symmetry. Although the two enantiomers can be interconverted by relative rotation of the rings, they are prevented from doing so by the bulk of the Si^{i}Pr$_3$ substituents.

The complexes, [M(η^8-C_8H_4{1,4-Si^{i}Pr$_3$}$_2$)$_2$] (M = Th, U) are simply prepared by reaction of $ThCl_4$ or UCl_4 and K_2[C_8H_4{1,4-Si^{i}Pr$_3$}$_2$)$_2$] in THF at room temperature. Cloke has shown the presence of two isomers of [Th(η^8-C_8H_4{1,4-Si^{i}Pr$_3$}$_2$)$_2$] in a single crystal (Figure 1).[5] They differ in the relative faces of the rings presented to the thorium and in the twist angles (as defined by the angle between the two bridgehead C−C vectors) of the two pentalene rings. The latter are 83° and 38° for isomers

[†] University of Sussex.
[‡] University of Oxford.

(1) Miyake, A.; Kanai, A. *Angew. Chem., Int. Ed. Engl.* **1971**, *10*, 1.
(2) Bunel, E. E.; Valle, L.; Jones, N. L.; Carroll, P. J.; Barra, C.; Gonzalez, M.; Munoz, M.; Visconti, G.; Aizman, A.; Manriquez, J. M. *J. Am. Chem. Soc.* **1988**, *110*, 6597.
(3) Knox, S. A. R.; Stone, F. G. A. *Acc. Chem. Res.* **1974**, *7*, 321.
(4) Kuchta, M. C.; Cloke, F. G. N.; Hitchcock, P. B. *Organometallics* **1998**, *17*, 1934, and references therein.
(5) Cloke, F. G. N.; Hitchcock, P. B. *J. Am. Chem. Soc.* **1997**, *119*, 7899.
(6) Jonas, K.; Gabor, G.; Mynott, R.; Angermund, K.; Heinemann, O.; Kruger, C. *Angew. Chem., Int. Ed. Engl.* **1997**, *36*, 1712.
(7) Jonas, K.; Kolb, P.; Kollbach, G.; Gabor, B.; Mynott, R.; Angermund, K.; Heinemann, O.; Kruger, C. *Angew. Chem., Int. Ed. Engl.* **1997**, *36*, 1714.

10.1021/om9807912 CCC: $18.00
Publication on Web 02/25/1999

1a and 1b, respectively and appear to be controlled by minimization of steric repulsion between the bulky Si^iPr_3 groups. The two forms are not interconvertable by ligand rotation but only by removing one ligand and presenting the opposite face to the metal. 1a would have S_4 symmetry if the twist angle were 90°, whereas 1b is chiral with D_2 symmetry. Solution NMR showed that the two isomers persisted in solution, and no evidence could be found for any interconversion.

This work examines the electronic structure of the bispentalene f-block complexes $[M(\eta^8\text{-}C_8H_4\{1,4\text{-}Si^iPr_3\}_2)_2]$ (M = Th **1**, U **2**), utilizing photoelectron spectroscopy and density functional calculations. It elucidates the key factors leading to the adoption of the bis-η^8 geometry and assesses the role of f orbitals in bonding.

Experimental Section

Compound **1** was synthesized by published procedures[5] and **2** in a similar manner from UCl_4.

Synthesis of $K_2[C_8H_4(1,4\text{-}Si^iPr_3)_2]$. (a) Cyclooctatetraene (11.3 g, 0.108 mol) in a slow stream (1.5 $cm^3\ min^{-1}$ at STP) of dinitrogen was passed through a quartz tube at 615 ± 1 °C under a controlled dynamic vacuum of 1.0 ± 0.05 mbar over a period of 24 h in a flash vacuum pyrolysis apparatus; the resultant mixture of dihydropentalenes was collected in a trap at −78 °C.[8] The latter was then dissolved in precooled (−78 °C) hexane (100 cm^3) and DME (23 cm^3, 0.22 mol) added, followed by $LiBu^n$ (2.5 M in hexanes, 88 cm^3, 0.22 mol) dropwise with stirring, which resulted in the precipitation of white $[Li(DME)]_2[C_8H_6]$.[9] After warming the mixture to room temperature, the latter was isolated by filtration on a frit, washed with hexane (3 × 50 cm^3), and dried under vacuum. Yield: 27.8 g, 87% based on cyclooctatetraene.

NMR data (THF-d_8, 295 K, Bruker DMX300): ^{1}H δ 5.76 (t, 2H, ring C*H*, J_{HH} 3.0), 5.00 (d, 4H, ring C*H*, J_{HH} 3.0), 3.42 (s, 8H, DME CH_2), 3.27 (s, 12H, DME CH_3); ^{7}Li{^{1}H} δ −8.57 (s).

(b) Tri(isopropylsilyl) triflate (6.12 g, 20 mmol) was added dropwise to a stirred solution of $[Li(DME)]_2[C_8H_6]$ (2.95 g, 10 mmol) in THF (100 cm^3) at −78 °C; the mixture was then allowed to warm to 0 °C and the solvent removed under reduced pressure at this temperature. The resultant white solid was extracted with pentane (3 × 100 cm^3) and filtered, and the pale yellow filtrate was concentrated and cooled to −40 °C to afford white crystals of $[C_8H_6(1,4\text{-}Si^iPr_3)_2]$. These were collected and washed with pentane (2 × 10 cm^3) at −78 °C. Yield: 3.2 g, 77%.

HRMS (EI): 416.330 456 (calculated 416.329 459)

NMR data (benzene-d_6), 295 K, Bruker DMX300): ^{1}H δ 6.82 (d, 2H, ring C*H*, J_{HH} 4.8), 6.65 (d, 2H, ring C*H*, J_{HH} 4.8), 3.56 (s, 2H, ring C*H*), 1.12 (m, 6H, ^{i}Pr−C*H*), 1.08 (d, 18H, ^{i}Pr−CH_3, J_{HH} 6.4, 1.01 (d, 18H, ^{i}Pr−CH_3, J_{HH} 6.4); ^{13}C{^{1}H} δ 153.0 (ring-*C*), 134.3 (ring-*C*H), 127.9 (ring-*C*H), 39.7 (ring-*C*H-Si^iPr_3), 19.3 (^{i}Pr−CH_3), 19.1 (^{i}Pr−CH_3), 12.7 (^{i}Pr−*C*H).

(c) Diethyl ether, precooled to −78 °C, was added to a stirred, solid mixture of $[C_8H_6(Si^iPr_3\text{-}1,5)_2]$ (2.08 g, 5 mmol) and $[KNH_2]$ (0.55 g, 10 mmol) in a −78 °C bath and the mixture allowed to warm to room temperature overnight. The resultant orange solution was then filtered from small amounts of insoluble material and evaporated to dryness under reduced pressure to afford off-white $K_2[C_8H_4(1,4\text{-}Si^iPr_3)_2]$ in essentially quantitative yield.

NMR data (benzene-d_6), 295 K, Bruker DMX300): ^{1}H δ 6.41 (d, 2H, ring C*H*, J_{HH} 3.2), 5.80 (d, 2H, ring C*H*, J_{HH} 3.2), 1.45 (m, 6H, ^{i}Pr−C*H*, J_{HH} 7.1), 1.28 (d, 36H, ^{i}Pr−CH_3, J_{HH} 7.1); ^{13}C{^{1}H} δ 139.2 (ring-*C*), 121.6 (ring-*C*H), 94.1 (ring-*C*H), 79.5 (ring-*C*Si^iPr_3), 20.5 (^{i}Pr−*C*H_3), 13.6 (^{i}Pr−*C*H); ^{29}Si{^{1}H} δ 4.19 (*Si*^{i}Pr$_3$).

Synthesis of $[U\{C_8H_4(1,4\text{-}Si^iPr_3)_2\}_2]$, 2. THF (75 cm^3), precooled to −78 °C, was added to mixture of solid $[UCl_4]$ (0.379 g, 1 mmol) and solid $K_2[C_8H_4(1,4\text{-}Si^iPr_3)_2]$ (0.984 g, 2 mmol), and the resultant suspension stirred overnight at room temperature. The solvent was then removed under reduced pressure and the residue extracted with pentane (150 cm^3) and filtered through Celite on a frit. Concentration of the green-brown filtrate and slow cooling to −50 °C afforded deep green-brown crystals of **2**, which were washed with cold (−78 °C) pentane and dried under vacuum. Yield: 0.74 g, 70%.

MS (EI): *m*/*z* 1066 (100%) (M^+).

Anal. Found: C 58.93; H 9.00. Calcd for $[C_{52}H_{92}Si_4U]$: C 58.50; H 8.68.

NMR data (toluene-d_8, 295 K, Bruker DMX300): ^{1}H δ 16.7 (brs, 2H, ring C*H*), −12.1 (brs, 2H, ring C*H*), −33.9 (brs, 2H, ring C*H*), −63.4 (brs, 2H, ring C*H*), −4.4 (brm, 12H, ^{i}Pr−C*H*), −1.4 (brs 18H, ^{i}Pr−CH_3), −2.2 (brs 18H, ^{i}Pr−CH_3), −4.8 (brs 18H, ^{i}Pr−CH_3), −7.3 (brs 18H, ^{i}Pr−CH_3); ^{13}C{^{1}H} δ 651.1 (ring-*C*), 602.0 (ring-*C*), 540.1 (ring-*C*H), 468.8 (ring-*C*H), 419.6 (ring-*C*), 331.6 (ring-*C*), 264.0 (ring-*C*H), 178.0 (ring-*C*H), 26.6 (^{i}Pr−*C*H), 19.6 (^{i}Pr−*C*H), 13.2 (^{i}Pr−*C*H_3), 12.4 (^{i}Pr−*C*H_3), 6.5 (^{i}Pr−*C*H_3), 3.8 (^{i}Pr−*C*H_3); ^{29}Si{^{1}H} δ −101.26 (*Si*^{i}Pr$_3$), −133.89 (*Si*^{i}Pr$_3$).

Photoelectron Spectroscopy. He I and He II photoelectron spectra of **1** and **2** were recorded using a PES Laboratories Ltd. 0078 spectrometer interfaced with an Atari microprocessor. The spectra were calibrated using He, Xe, and N_2. Solution NMR on a sublimed sample of **1** shows that the isomer ratio remains unchanged, hence it is considered likely that both isomers are present in the gas-phase sample.

Theoretical Methods. Density functional calculations were performed to optimize the ground-state structure and to aid spectral assignment. The structure $M(pent)_2$ (M = Th, U; pent = η^8-C_8H_6) was used as a model for $[M(\eta^8\text{-}C_8H_4\{1,4\text{-}Si^iPr_3\}_2)_2]$ to save computational time. All calculations were performed using density functional methods of the Amsterdam Density Functional package (Version 2.3).[10] The basis set used triple-ζ accuracy sets of Slater-type orbitals, with relativistic corrections and with a single polarization function added for the main group atoms: 2p on hydrogen and 3d on carbon atoms. The relativistic cores of the atoms were frozen: carbon up to the 1s orbital, and thorium and uranium to the 5d orbitals. The GGA (nonlocal) method was used, using Vosko, Wilk, and Nusair's local exchange correlation[11] with nonlocal exchange corrections by Becke[12] and nonlocal correlation corrections by Perdew.[13] A summary of calculations performed is given in Table 1.

Results and Discussion

1. General Bonding Considerations. The pentalene dianion ($pent^{2-}$) being aromatic is planar in the uncoordinated state. The phases of the π orbitals of pentalene are shown in Figure 2. The pentalene dianion is formally related to $C_8H_8^{2-}$ by loss of two hydrogens and formation of a C−C bond across the eight-membered ring. Consequently the π orbitals of $C_8H_6^{2-}$ may be correlated with those of $C_8H_8^{2-}$. Such a correlation is given in Table 2. The π_4 orbital of $C_8H_6^{2-}$ is stabilized with respect to the e_{2u} orbital of $C_8H_8^{2-}$, because the interaction between the π orbitals across the bridgehead is bonding, whereas π_3 of $C_8H_6^{2-}$ is destabilized with

(8) Meier, H.; Pauli, A.; Kochhan, P. *Synthesis* **1987**, 573.
(9) Stezowski, J. J.; Hoier, H.; Wilhelm, D.; Clark, T.; von Ragué Schleyer, P. J. *J. Chem. Soc., Chem. Commun.* **1985**, 1263.
(10) te Velde, G.; Baerends, E. J. *J. Comput. Phys.* **1992**, *99*, 84.
(11) Vosko, S. H.; Wilk, L.; Nusair, M. *Can. J. Phys.* **1990**, *58*, 1200.
(12) Becke, A. D. *Phys. Rev.* **1988**, *A38*, 2398.
(13) Perdew, J. P. *Phys. Rev.* **1985**, *B33*, 8822.

Table 1. Summary of Calculations Performed on M(pent)$_2$

structure	calculation	symmetry	electronic structure
[Th(η^8-C_8H_6)$_2$]	geometry optimization frequency calculation	D_{2d}	not constrained
[Th(η^8-C_8H_6)$_2$]$^+$	single point	D_{2d}	$10e^4 8a_1^2 8b_2^2 4b_1^2 4a_2^1$ $10e^4 8a_1^2 8b_2^2 4b_1^1 4a_2^2$ $10e^4 8a_1^2 8b_2^1 4b_1^2 4a_2^2$ $10e^4 8a_1^1 8b_2^2 4b_1^2 4a_2^2$ $10e^3 8a_1^2 8b_2^2 4b_1^2 4a_2^2$
[Th(η^8-C_8H_6)$_2$]	geometry optimization frequency calculation linear transit	D_2	not constrained
[*trans*-Th(η^5-C_8H_6)$_2$]	geometry optimization	C_{2h}	not constrained
[*cis*-Th(η^5-C_8H_6)$_2$]	geometry optimization	C_{2v}	not constrained
[U(η^8-C_8H_6)$_2$]	geometry optimization	D_{2d}	constrained to triplet state
[U(η^8-C_8H_6)$_2$]$^+$	single point both quartet and doublet states	D_{2d}	$10e^4 8a_1^2 8b_2^2 4b_1^2 4a_2^2 11e^1$ $10e^4 8a_1^2 8b_2^2 4b_1^2 4a_2^1 11e_1^2$ $10e^4 8a_1^2 8b_2^2 4b_1^1 4a_2^2 11e_1^2$ $10e^4 8a_1^2 8b_2^1 4b_1^2 4a_2^2 11e_1^2$ $10e^4 8a_1^1 8b_2^2 4b_1^2 4a_2^2 11e_1^2$ $10e^3 8a_1^2 8b_2^2 4b_1^2 4a_2^1 11e_1^2$

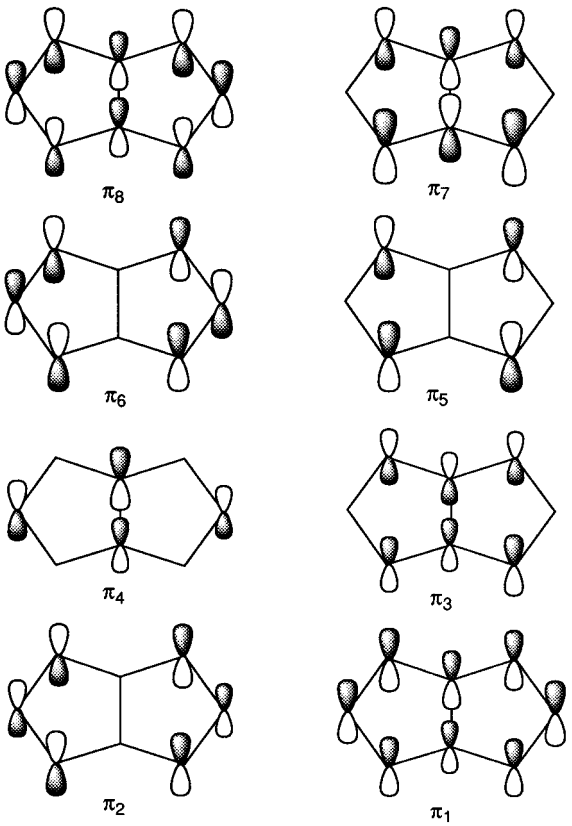

Figure 2. Representations of the pentalene dianion molecular orbitals of π symmetry. The numbering indicates the energy ordering, and the phases of the orbitals give the number of nodes.

respect to the e_{1g} orbitals of $C_8H_8^{2-}$, because, in this case, the interaction across the bridgehead is antibonding.

For simplicity the M(C_8H_6)$_2$ framework is treated with D_{2d} symmetry. The symmetry adapted linear combinations (SALCs) of the pentalene π orbitals when combined in D_{2d} symmetry are listed in Table 2 and shown in the generalized MO diagram presented in Figure 3. An actinide may bond to a_1, b_1, b_2, and e_1 SALCs through its d orbitals and a_1, a_2, b_2, and e_1 SALCs through its f orbitals. It is thus reasonable to assume that the orbital ordering follows that of the ligand, that, given the relative efficacy of d and f orbitals in covalent

Table 2. Correlation of Occupied π Orbitals of $C_8H_8^{2-}$ with Those of $C_8H_6^{2-}$, $(C_8H_6^{2-})_2$, and M

$C_8H_8^{2-}$ D_{8h}	$C_8H_6^{2-}$	$(C_8H_6^{2-})_2$ D_{2d}	M
a_{2u}	π_1	a_1	s, d (z^2), f (xyz)
		b_2	p (z), d (xy), f (z^3)
e_{1g}	π_2	e	p (x, y), d (xz, yz), f (xy^2, x^2y) (xz^2, yz^2)
	π_3	e	p (x, y), d (xz, yz), f (xy^2, x^2y) (xz^2, yz^2)
e_{2u}	π_4	a_1	s, d (z^2)
		b_2	p (z), d (xy), f (z^3)
	π_5	b_1	d (x^2-y^2)
		a_2	f ($z(x^2-y^2)$)

bonding, the highest occupied molecular orbital (HOMO) of **1** is of a_2 symmetry and has an Th f contribution, and that the second occupied molecular orbital (HOMO-1) is of b_1 symmetry and has a Th d contribution.

2.1. Structural Studies. The size of **1** and **2** with their large substituents is so computationally demanding that calculations were instead performed on M(pent)$_2$ with M = Th and U. Although the isomers found for **1** are of low symmetry, the closeness of the molecular frameworks to D_{2d} and D_2 symmetry made structures with these symmetry constraints reasonable models; again the advantage is the reduced computational time and the relative ease of calculating ionization energies when the symmetry is high.

The substantial NMR chemical shifts found for **2** show it to be paramagnetic, as is the case for all known U(IV) compounds. Geometry optimization of U(pent)$_2$ was therefore carried out on the molecule with D_{2d} symmetry in a triplet state. SCF convergence was difficult to achieve for this compound as a result of the closeness in energy of the f orbitals. The configuration was therefore fixed to be the same as the Th compound with, in addition, the two extra electrons occupying a degenerate pair of orbitals with e symmetry. Convergence was readily achieved under this constraint.

Two geometry optimizations of Th(pent)$_2$ under D_{2d} and D_2 symmetry constraints yielded bond lengths and angles given in Table 3. Agreement between theory and experiment is very good. The D_{2d} structure for Th was found to lie 0.043 eV (4.1 kJ mol^{-1}) higher in energy than the D_2 structure. A frequency calculation on the D_{2d} optimized structure showed it to have one negative force constant with an imaginary frequency of 64i cm^{-1}.

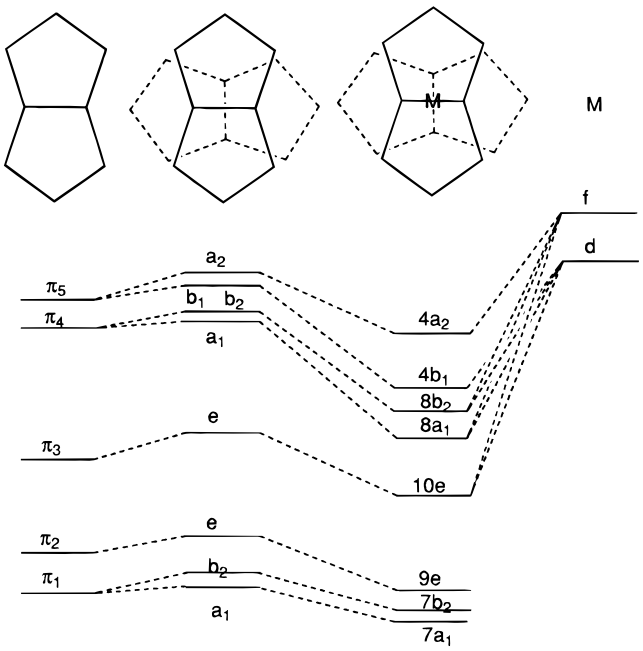

Figure 3. MO diagram for Th(pent)$_2$. Energies are taken from the fragment calculation. The left-hand column gives the energies of the first five π orbitals of pentalene and the second column those of the related orbitals when two pentalene ligands are combined in the geometry they have in the D_{2d} complex. The third column gives the MO energies in the D_{2d} complex and the right-hand column the energies assumed in the calculation for the d and f orbitals of the metal.

The associated vibrational mode corresponded to relative rotation of the two pentalene ligands.

To test the stability of an η^5 coordination mode, geometry optimizations were also carried out for *trans*-Th(η^5-C_8H_6)$_2$ and *cis*-Th(η^5-C_8H_6)$_2$ under C_{2h} and C_{2v} constraints, respectively. Both reverted to a lower energy D_{2h} Th(η^8-C_8H_6)$_2$ structure, showing the preference for η^8 coordination of the pentalene ligand. The optimized D_{2h} structure was found to lie 0.21 eV (20.3 kJ mol^{-1}) above the D_{2d} structure. Examination of the model indicated that the D_{2h} geometry is destabilized by steric interactions between the wing tip hydrogens.

The barrier to relative rotation of the two ligands was investigated further by means of a linear transit run in which the relative orientation of the two pentalene ligands was fixed at values between 0° and 90° but all other geometric variables were optimized. Again D_2 symmetry was assumed. The results are given in Table 4. They confirm the results from the optimization studies.

Repeated attempts to obtain a D_2 structure with no negative force constants failed. Small imaginary frequencies corresponding to relative rotation of the pentalenes were obtained. This is attributed to the very flat energy surface for relative ring rotation.

The calculated energies suggest little electronic preference between the ring conformations found for the isomers 1a and 1b. The ring conformations are almost certainly controlled by steric interactions between the bulky substituents as suggested by Cloke,[5] although the calculations do suggest that an eclipsed arrangement of the rings would be disfavored.

U(pent)$_2$, optimized with a D_{2d} symmetry constraint, was calculated to have shorter metal−carbon distances than the thorium compound (Table 3), but otherwise the optimized structure was very similar.

2.2. Orbital Structure. Selected orbital energies of the DFT calculations with optimized geometries are presented in Table 5. Those from the D_{2d} calculation on Th(pent)$_2$ were used to construct the MO diagram shown in Figure 3. A fragment calculation and Mulliken population analysis were used to assess the metal and ligand contents of the upper filled orbitals (Table 6).

Isosurfaces for the four highest occupied orbitals of Th(pent)$_2$ (D_{2d} structure) are shown in Figure 4. Lower orbitals are mainly ligand π orbital in character. The top two orbitals, 4a$_2$ and 4b$_1$, involve the metal binding exclusively to the α carbons through f and d orbitals, respectively. The contribution of the Th 6d to 4b$_1$ is 24%, while that of Th 5f to 4a$_2$ is less, at 14%. The 4b$_1$ orbital is estimated to be 0.67 eV more stable than the 4a$_2$. Thus the Th 6d orbitals are more effective at covalent bonding than the Th 5f, as was found for the analogous thoracene and uranocene.[14,15] The next two orbitals, 8b$_2$ and 8a$_1$, where both d and f orbitals can contribute to the bonding, both show greater d than f character. It is through these two orbitals that interaction with the bridgehead and wingtip carbons takes place. Overall metal ligand mixing is lower in this orbital pair. The covalent interaction shown in these four orbitals is presumably the driving force behind the ligand folding. The fold ensures that all ring carbon atoms are within bonding distance of the metal.

The D_2 structure, whch is twisted from the D_{2d} by 48.5°, gives rise to spatially similar orbitals which differ in energy from their D_{2d} analogues by up to 0.3 eV.

The uranium complex is calculated to have an orbital structure similar to the thorium complex, but in addition there are two f electrons; these were constrained to occupy orbitals of e symmetry lying 1.7 eV above the 4a$_2$ orbital. In actinides spin−orbit effects are likely to dominate the ground-state structure, being greater than ligand field effects. A spin−orbit calculation was also carried, out and in this case one f electron occupied an orbital with $j = 3/2$ (−3.23 eV) and the other an orbital with $j = 1/2$ (−3.19 eV). However, a U^{4+} ion has a ground state with $J = 4$, and ligand field effects may be insufficient to quench this angular momentum. It should be noted that in the spin−orbit calculation other f orbitals lie close to the HOMO in energy and a single configurational description of the ground state of U(pent)$_2$ is likely to be inadequate.

3.1. Photoelectron Spectra. The He I and He II photoelectron spectra of **1** and **2** are presented in Figure 5, and the vertical ionization energies (IE) and band assignments are shown in Table 7.

Both compounds show ill-defined bands in the region 6.3−8.0 eV (A−D). These bands show an increase in intensity relative to band E on going from He I to He II radiation and are thus assigned to metal−ligand bonding orbitals, 4a$_2$, 4b$_1$, 8b$_2$, and 8a$_1$. All spectra also show a band (E) at ca. 9 eV, which is assigned to the

(14) Clark, J. P.; Green, J. C. *J. Chem. Soc., Dalton Trans.* **1977**, 505.
(15) Brennan, J. G.; Green, J. C.; Redfern, C. M. *J. Am. Chem. Soc.* **1989**, *111*, 2373.

Table 3. Experimental Structural Parameters for 1 and Predicted Structural Parameters for M(pent)$_2$ (M = Th, Ce, and U) (Å and deg)

parameter (Å or deg)	**1**	Th(pent)$_2$ D_{2d}	Th(pent)$_2$ D_2	U(pent)$_2$ D_{2d}
ligand torsion	83, 38	90	48.5	90
M−C(bridge)	2.543(10), 2.55(2)	2.51	2.51	2.43
M−C(α)	2.797(11), 2.748(10)	2.71	2.70	2.62
	2.78(2), 2.75(2)	2.71		
M−C(*β*)	2.908(11), 2.88(2)	2.84	2.84	2.74
ligand fold	24	26.5	26.5	29.8
C(bridge)−C(bridge)	1.39(2), 1.47(3)	1.45	1.45	1.45
C(bridge)−C(α)	1.41(2), 1.43(2), 1.49(2)	1.42	1.43	1.42
			1.43	
C(α)-C(*β*)	1.46(2), 1.36(2), 1.43(2)	1.41	1.41	1.41
			1.40	

Table 4. Energy of D_2 Structure Relative to D_{2d} Structure (ΔE) for Th(pent)$_2$ as a Function of the Relative Orientation (θ) of the Two Pentalene Ligands

	θ (deg)						
	90	75	60	45	30	15	0
ΔE (eV)	0.00	0.00	−0.04	−0.01	0.07	0.19	0.21

Table 5. Orbital Energies (eV) of M(pent)$_2$

				U(pent)$_2$ D_{2d}		
Th(pent)$_2$ D_{2d}		Th(pent)$_2$ D_2			energy	
orbital	energy	orbital	energy	orbital	spin α	spin *β*
				$11e_1$	−3.27	
$4a_2$	−4.90	$12b_1$	−5.18	$4a_2$	−5.22	−5.06
$4b_1$	−5.61	12a	−5.34	$4b_1$	−5.70	−5.64
$8b_2$	−6.08	$11b_1$	−5.98	$8b_2$	−6.28	−6.12
$8a_1$	−6.40	11a	−6.47	$4a_1$	−6.57	−6.44
$10e_1$	−7.10	$10b_3$	−6.84	$10e_1$	−7.15	−7.08
		$10b_2$	−7.39			
$9e_1$	−8.37	$9b_2$	−8.17	$11e_1$	−8.31	−8.26
		$9b_3$	−8.46			
$7b_2$	−8.48	$10b_1$	−8.46	$7b_2$	−8.44	−8.41
$7a_1$	−8.69	10a	−8.67	$7a_1$	−8.71	−8.70

Table 6. Mulliken Population Analysis of the Contributions of the Metal and Ligand Orbitals to the Upper Occupied MO of Th(pent)$_2$ (D_{2d})

	Th(pent)$_2$			
MO	Th AO	Th %	ligand orbital	ligand %
$4a_2$	f ($z(x^2-y^2)$)	14.4	π_5	83.7
$4b_1$	d (x^2-y^2)	24.0	π_5	74.3
$8b_2$	p (z)	0.6	π_4	82.6
	d (xy)	9.0		
	f (z^3)	5.8		
$8a_1$	d (z^2)	13.3	π_4	78.9
	f (xyz)	1.9		
$10e_1$	p (x, y)	2.7	π_3	79.9
	d (xz, yz)	4.3	π_2	8.5
	f (xz^2, yz^2)	2.4		
	f (xy^2, x^2y)	0.1		
$9e_1$	p (x, y)	1.0	π_2	80.6
	d (xz, yz)	9.1		
	f (xz^2, yz^2)	0.2		
	f (xy^2, x^2y)	0.1		
$7b_2$	p (z)	1.3	π_1	90.8
	d (xy)	0.3		
	f (z^3)	0.5		
$7a_1$	d (z^2)	1.0	π_1	97.1

ionization of Si−C bonding electrons. This is in agreement with the photoelectron spectra of other compounds containing Si−C linkages.[16,17] The spectrum of **2** also

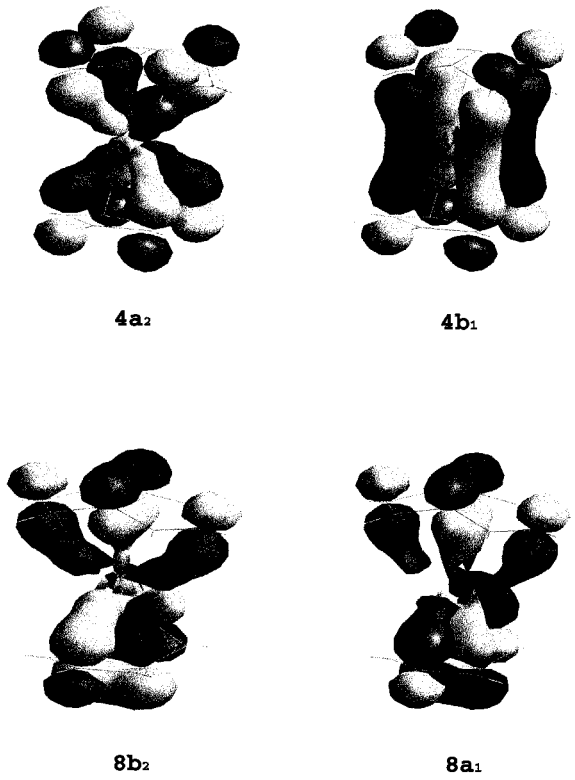

Figure 4. Isosurfaces for the four highest occupied orbitals of Th(pent)$_2$ with D_{2d} symmetry.

contains a band at 5.79 eV (X). This increases dramatically in intensity in the He II spectrum, supporting the assignment to ionization from a pure metal f orbital.

In the PE spectrum of thoracene and uranocene the separation of the bands associated with the e_{2u} and e_{2g} metal ligand bonding orbitals is much superior to that found for the pentalene complexes.[14,15] In the former cases it is possible to see differential intensity changes between these bands, the e_{2u} band gaining more intensity in the He II spectrum than the e_{2g} band as a result of the f orbital contribution. No such differential intensity changes were detectable among the bands A−D of the pentalene complexes. It is likely that the presence of the two isomers in the crystal and hence in the gas phase is partly responsible for the poor definition of the spectral bands. Their differing symmetry about the metal center leads to frontier orbitals of slightly different energy (see Table 5) and consequently different ionization energies resulting in the broad unresolved ionization band that we observe. Also the lower symmetry of the D_2 isomer means that f−d mixing is allowed in the top two occupied orbitals. Thus the

(16) Evans, S.; Green, J. C.; Joachim, P. J.; Orchard, A. F.; Turner, D. W.; Maier, J. P. *J. Chem. Soc., Faraday Trans. 2* **1972**, *68*, 1161.
(17) Evans, S.; Green, J. C.; Jackson, S. E. *J. Chem. Soc., Faraday Trans. 2* **1973**, *69*, 191.

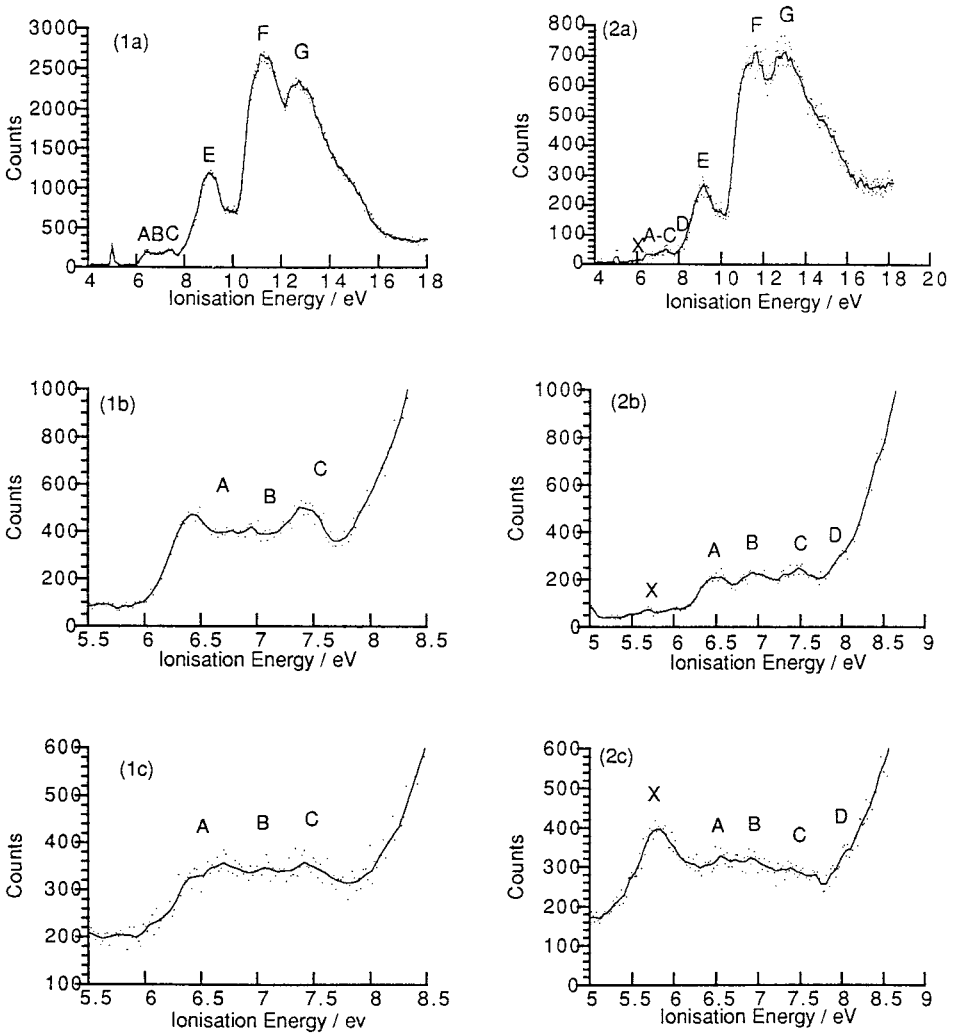

Figure 5. PE spectra of **1**: (a) He I full range, (b) He I low IE range, (c) He II low IE range. PE spectra of **2**: (a) He I full range, (b) He I low IE range, (c) He II low IE range.

Table 7. Experimental IE of 1 and 2 and Predicted IE for M(pent)$_2$ (M = Th and U) with D_{2d} Symmetry

				U(pent)$_2$	
orbital	**1**	Th(pent)$_2$	**2**	spin α	spin β
$11e_1$	n/a	n/a	5.79	5.75	n/a
$4a_2$	6.40	6.65	6.48	7.17	*a*
$4b_1$	6.93	7.32	6.93	7.51	7.46
$8b_2$	7.43	7.83	7.48	8.08	7.95
$8a_1$	hidden by Si−C	8.13	8.06 (sh)	8.38	8.26
$10e_1$	hidden by Si−C	8.88	hidden by Si−C	9.02	8.95

[a] SCF convergence failed for this state.

overlapping nature of the PE band and the lack of pronounced relative intensity change is understandable.

The uranium compound, **2**, shows an additional band at 5.79 eV, which shows a significant increase in relative intensity in the He II spectrum consistent with ionization of an f electron. As with other U(IV) compounds, only one f band is observed. Egdell et al. have discussed the final state structure in the PE spectra of U(IV) compounds.[18] From the $J = 4$ ground term of U^{4+} $^2F_{7/2}$ and $^2F_{5/2}$ ion states are in principle accessible. The PE intensities of the two final states depend on the atomic coupling scheme. In a Russell−Saunders limit the predicted $^2F_{5/2}$:$^2F_{7/2}$ intensity ratio is 1.714:0.286. For pure j−j coupling only the $^2F_{5/2}$ is accessible. It is likely, therefore, that the observed f band corresponds to a $^2F_{5/2}$ unsplit ion state.

The f ionization of **2** at 5.79 eV is of significantly lower energy than that of uranocene at 6.2 eV. It has a similar value to that of octamethyl uranocene (5.73 eV).[19] It is also significantly lower than that of U(η-C_5H_5)$_4$, which shows an f band at 6.34 eV.[20] The highest lying ligand levels in the pentalene complexes also have lower IE than the related cyclooctateraenyl and cyclopentadienyl complexes of both Th and U.[14,20] Thus pentalene appears to be a better donor than cyclooctatetraene or two cyclopentadienyl ligands.

3.2. Calculation of Ionization Energies. The IEs of Th(pent)$_2$ and U(pent)$_2$ (D_{2d} symmetry) were calculated by subtracting the energy of the ground-state molecule from that of the required ion state. The results are shown in Table 7.

It must be noted that computed ionization energies neglect the effect of the Si^{i}Pr$_3$ groups, in terms of both their electronic effect and their steric distortions away

(18) Downs, A. J.; Egdell, R. G.; Orchard, A. F.; Thomas, P. D. P. *J. Chem. Soc., Dalton Trans.* **1978**, 1755.

(19) Green, J. C.; Payne, M. P.; Streitwieser, A., Jr. *Organometallics* **1983**, *2*, 1707.

(20) Green, J. C.; Kelly, M. R.; Long, J. A.; Kanellakopulos, B.; Yarrow, P. I. W. *J. Organomet. Chem.* **1981**, *212*, 329.

from D_{2d} symmetry. Nevertheless, within these limitations agreement is very good, both confirming the assignments and producing experimental support for the nature of the orbital interactions described above.

Conclusions

Density functional calculations of the geometry and PE spectra of $Th(pent)_2$ and $U(pent)_2$ are in excellent agreement with experimental data on **1** and **2**.

The HOMO of the pentalene dianion is an orbital of δ symmetry with respect to an η^8-coordinated metal. In bispentalene complexes actinides provide both 5f and 6d orbitals that can overlap with the symmetry adapted linear combinations of these pentalene HOMOs and form covalent bonds. The HOMO-1 of the pentalene dianion is also able to form bonds with metal d and f orbitals, but the metal makes a smaller contribution in these cases. Overall, the 6d orbitals make a larger contribution to bonding than the 5f. Optimization of the metal−carbon distances for covalent interaction involves a folding of the pentalene dianion at the bridgehead carbon. The decrease in f band IE along the series $U(\eta^5\text{-}C_5H_5)_4 > U(\eta^8\text{-}C_8H_8)_2 > U(\eta^8\text{-}C_8H_4\{1,4\text{-}Si^iPr_3\}_2)_2$ indicates an increase in donor power of the ligands.

Acknowledgment. We thank EPSRC for a studentship (C.N.J.).

OM9807912